# Reverse Shocks in Short Gamma-Ray Bursts

## – The case of GRB 160821B and prospects as gravitational-wave counterparts –

Gavin P Lamb[1]

[1] School of Physics and Astronomy, University of Leicester, University Road, Leicester, LE1 7RH, UK
*E-mail: gpl6@leicester.ac.uk*

Abstract

The shock system that produces the afterglow to GRBs consists of a forward- and a reverse-shock. For short GRBs, observational evidence for a reverse-shock has been sparse – however, the afterglow to GRB 160821B requires a reverse-shock at early times to explain the radio observations. GRB 160821B is additionally accompanied by the best sampled macronova without a gravitational-wave detection, and an interesting late time X-ray afterglow behaviour indicative of a refreshed-shock. The presence of an observed reverse-shock in an on-axis short GRB means that the reverse-shock should be considered as a potential counterpart to gravitational-wave detected mergers. As a gravitational-wave counterpart, the afterglow to an off-axis GRB jet can reveal the jet structure – a reverse-shock will exist in these structured jet systems and the signature of these reverse-shocks, if observed, can indicate the degree of magnetisation in the outflow. Here we show the case of GRB 160821B, and how a reverse-shock will appear for an off-axis observer to a structured jet.

Key words: Yamada conference LXXI: proceedings — gamma-ray bursts: GRB 160821B, general — gravitational wave: electromagnetic counterparts

## 1. Introduction

For a relativistic shell expanding into a medium, two shocks will form; a forward shock that propagates into the external medium, and a reverse shock that propagates into the shell (Sari & Piran 1995). In describing the reverse shock, two regimes are usually discussed, these are the thin shell, or Newtonian shock case, and the thick shell, or relativistic shock case (Kobayashi 2000, etc). The relativistic shell will decelerate at the reverse shock crossing time in both regimes (Kobayashi et al. 1999). The duration and energetics of short gamma-ray bursts (GRBs) imply that any reverse shock in these systems will typically be described by the thin shell case (Lamb & Kobayashi 2018, 2019).

Emission from a reverse shock is an important probe of the conditions in a GRB outflow towards the central engine. Modelling the observed afterglow emission enables constraints to be placed on the magnetisation and the bulk Lorentz factor $\Gamma_0$, where $F_{max,r} = \Gamma_0 F_{max,f} C_F R_B$, and here $F_{max}$ is the maximum synchrotron flux from the reverse and forward shock, $r$ and $f$ respectively, $C_F$ is a correction factor, see Harrison & Kobayashi (2013), and $R_B \equiv \varepsilon_{B,r}/\varepsilon_{B,f}$ is the magnetisation parameter, see Zhang et al. (2003).

The reverse shock in short GRBs has been notoriously difficult to observe (Lloyd-Ronning 2018), however, the short GRB 051221A has evidence[1] of a reverse shock with a radio frequency detection and upper-limits (Soderberg et al. 2006), and recently reverse shock emission has been shown to be consistent with the optical afterglow to the candidate short GRB 180418A (Becerra et al. 2019), and radio observations of the afterglow to the short GRB 160821B require a reverse shock component (Lamb et al. 2019a; Troja et al. 2019a). These successes in observing the reverse shock in short GRBs, although rare, raise the prospect of identifying the reverse shock emission in gravitational-wave detected neutron star mergers, where the systems jet-axis is likely misaligned for an observer and so the afterglow and GRB will be observed off-axis (Lamb & Kobayashi 2017, 2018, 2019).

## 2. GRB 160821B

The short GRB 160821B, at a redshift of $z = 0.162$, had an isotropic gamma-ray energy of $E_{\gamma,iso} = (2.1 \pm 0.2) \times 10^{50}$ erg, based on the 8–10,000 keV band fluence of $(2.52 \pm 0.19) \times 10^{-6}$ erg cm$^{-2}$ (Lü et al. 2017). X-ray, opti-

*[1] GPL thanks Alexander van der Horst for kindly pointing out this paper in a comment following the conference talk

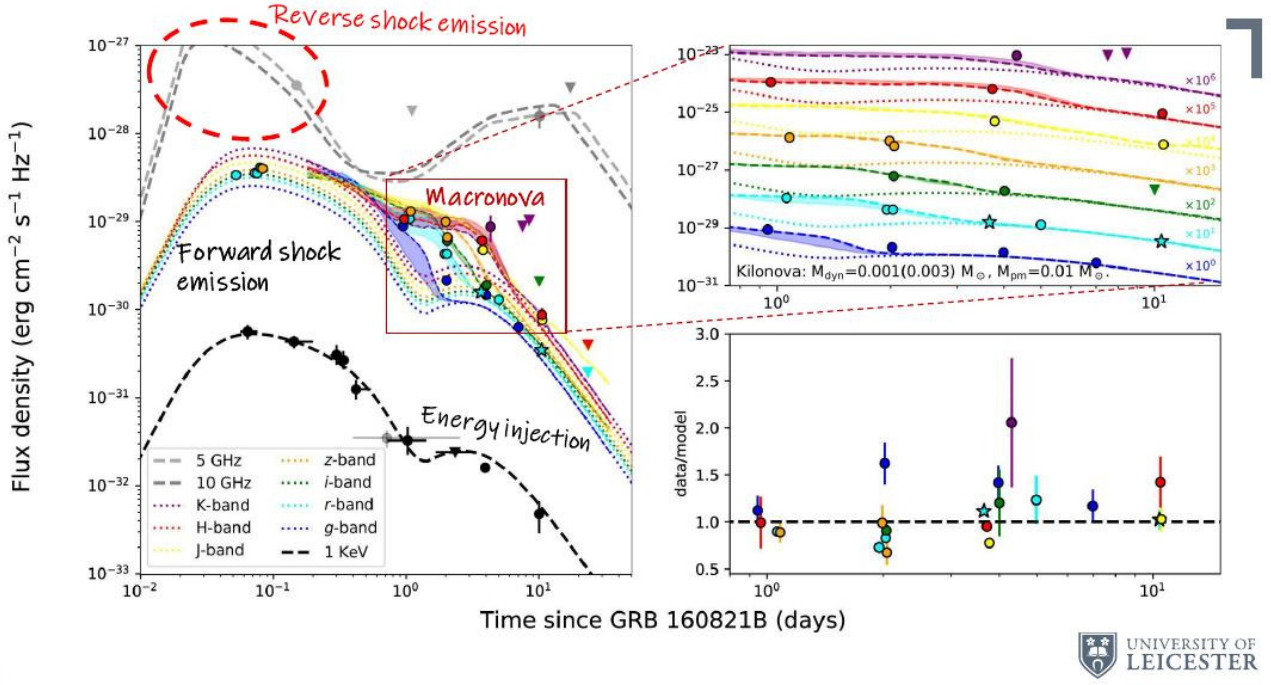


Fig. 1. The broadband afterglow to GRB 160821B. Dashed or dotted lines are the model light-curves, filled circles are data, and triangles upper-limits, see Lamb et al. (2019a) for details. Left: the afterglow from radio to X-ray frequencies (top to bottom), a reverse shock contribution is required at early times to explain the radio observation, while at late times energy injection is needed to explain the X-ray, optical and radio data. From $\sim$ 1–5 days an excess at optical and infrared indicates a macronova. Right top: expands the macronova and afterglow model with the data. Right bottom: shows the model fits versus data residual.

cal, and radio frequency observations of the afterglow to GRB 160821B were performed from 0.06–23.23 days after the burst; for a full list of the observations used here see Lamb et al. (2019a). Early infrared observations put limits on the presence of a macronova (Kasliwal et al. 2017), however, more complete broadband observations revealed emission at optical and infrared frequencies in excess of that expected from afterglow modelling of the X-ray and radio data (Lamb et al. 2019a; Troja et al. 2019a).

In Fig. 1 we show the afterglow data and our preferred model. The complex behaviour of the afterglow is explained variously by: the contribution of a reverse shock travelling into a mildly magnetised ($R_B \sim 8$) shell at early times ($\sim$ 0.1 days), we estimate a bulk Lorentz factor for the initial outflow $\Gamma_0 \sim 60$; a jet break at $\sim 0.3 - 0.4$ days followed by an injection of energy from a fallback powered second jet episode(Rosswog 2007; Kagawa et al. 2019)[2] that re-brightens the afterglow (Granot et al. 2003, etc); and a macronova contribution at $\sim 1-5$ days. The best-fitting macronova model (Kawaguchi et al. 2018) consists of two-components: a dynamical ejecta mass of $\sim 0.001\,M_\odot$, and a post-merger or secular ejecta mass of $\sim 0.01\,M_\odot$.

## 3. Reverse Shocks as Gravitational Wave Counterparts

The GRB 170817A and its macronova and afterglow in association with the gravitational-wave detected merger of a binary neutron star at $\sim$ 40 Mpc (Abbott et al. 2017) has shown that short GRBs are produced in binary neutron star mergers. The late-time afterglow to GRB 170817A indicated that the resultant jets from neutron star mergers, when viewed at a higher inclination than the central jet axis, will reveal the outflow structure (Lamb & Kobayashi 2017). The post-peak rapid decline of the late-time afterglow (Lamb et al. 2019b; Troja et al. 2019b), along with VLBI observations (Ghirlanda et al. 2019; Mooley et al. 2018), cleared any ambiguity in the jet-core dominated origin of the afterglow (Lamb et al. 2018).

For neutron star mergers discovered via gravitational-waves, the reverse shock in the afterglow can potentially be observed for systems that are inclined $< 20°$, at a luminosity distance $< 100$ Mpc, and that have some lateral structure; see Fig 2 and (Lamb & Kobayashi 2019). Additionally, a magnetisation parameter $R_B \sim$ a few is required and observations should ideally com-

*2 This second jet episode is slower than the initial GRB creating jet and likely responsible for the X-ray extended emission lasting $\sim$ 300s following the main burst

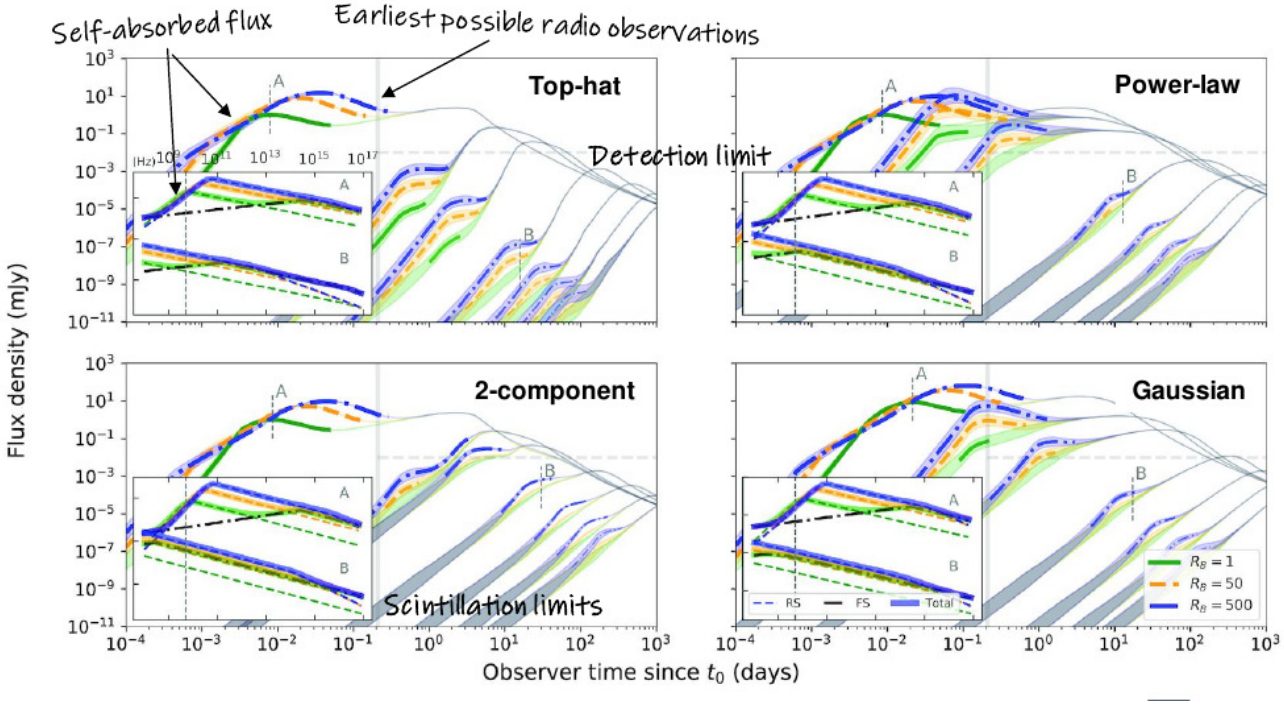


Fig. 2. The afterglow light-curve for four jet structure models following those in Lamb & Kobayashi (2017) but including sideways expansion, synchrotron self-absorption, and a reverse shock for an ejecta shell characterised by a magnetic parameter $R_B = [1, 50, 500]$, bold lines in green (solid), yellow (dashed), and blue (dash-dotted) respectively, see Lamb & Kobayashi (2019). The light-curves for an afterglow at 5 GHz and 100 Mpc are shown at $[0°, 12°, 18°, 36°, 54°, 72°, ]$ and $[90°]$. The effects of scintillation are shown with the grey shaded regions at early times while the size emitting region is still small (Granot & van der Horst 2014). Insets on each panel show the spectra at the times indicated by 'A' and 'B'.

mence at $\sim 0.1$ days post merger and at radio frequencies $< 100$ GHz. For such cases, scintillation may complicate the observations, however, carefully measured scintillation can be used to constrain the size of the emitting region (Granot & van der Horst 2014).

## References


Abbott, B. P., Abbott, R., Abbott, T. D., et al. 2017, ApJL, 848, L12
Becerra, R. L., Dichiara, S., Watson, A. M., et al. 2019, ApJ, 881, 12
Ghirlanda, G., Salafia, O. S., Paragi, Z., et al. 2019, Science, 363, 968
Granot, J., Nakar, E., & Piran, T. 2003, Nature, 426, 138
Granot, J., & van der Horst, A. J. 2014, PASA, 31, e008
Harrison, R., & Kobayashi, S. 2013, ApJ, 772, 101
Kagawa, Y., Yonetoku, D., Sawano, T., et al. 2019, ApJ, 877, 147
Kasliwal, M. M., Korobkin, O., Lau, R. M., et al. 2017, ApJL, 843, L34
Kawaguchi, K., Shibata, M., & Tanaka, M. 2018, ApJL, 865, L21
Kobayashi, S., Piran, T., & Sari, R. 1999, ApJ, 513, 669
Kobayashi, S. 2000, ApJ, 545, 807
Lamb, G. P., & Kobayashi, S. 2017, MNRAS, 472, 4953
Lamb, G. P., & Kobayashi, S. 2018, MNRAS, 478, 733
Lamb, G. P., Mandel, I., & Resmi, L. 2018, MNRAS, 481, 2581
Lamb, G. P., & Kobayashi, S. 2019, MNRAS, 489, 1820
Lamb, G. P., Tanvir, N. R., Levan, A. J., et al. 2019a, ApJ, 883, 48
Lamb, G. P., Lyman, J. D., Levan, A. J., et al. 2019b, ApJL, 870, L15
Lloyd-Ronning, N. 2018, Galaxies, 6, 103
Lü, H.-J., Zhang, H.-M., Zhong, S.-Q., et al. 2017, ApJ, 835, 181
Mooley, K. P., Deller, A. T., Gottlieb, O., et al. 2018, Nature, 561, 355
Rosswog, S. 2007, MNRAS, 376, L48
Sari, R., & Piran, T. 1995, ApJL, 455, L143
Soderberg, A. M., Berger, E., Kasliwal, M., et al. 2006, ApJ, 650, 261
Troja, E., Castro-Tirado, A. J., Becerra González, J., et al. 2019a, MNRAS, 489, 2104
Troja, E., van Eerten, H., Ryan, G., et al. 2019b, MNRAS, 489, 1919
Zhang, B., Kobayashi, S., & Mészáros, P. 2003, ApJ, 595, 950